Supplementary Material for

Synthesis, Properties and Highly Selective Mitochondria Staining with Novel, Stable and Superior Benzothiadiazole Fluorescent Probes

Brenno A. D. Neto,*[a] Pedro H. P. R. Carvalho,[a] Diego C. B. D. Santos,[a] Claudia C. Gatto,[a] Luciana M. Ramos,[a b] Nathalia M. de Vasconcelos,[a] José R. Corrêa,[a] Maísa B. Costa,[b] Heibbe C. B. de Oliveira,[a] and Rafael G. Silva[c]

[a] *Laboratory of Medicinal and Technological Chemistry, University of Brasília (IQ-UnB). Campus Universitário Darcy Ribeiro, CEP 70904970, P.O.Box 4478, Brasília-DF, Brazil; E-mail: brenno.ipi@gmail.com*

[b] *Laboratorio de Química Orgânica, IQ, UEG: UnUCET, Anápolis-Go,Brasil.*

[c] *Department of Biochemistry, Albert Einstein College of Medicine of Yeshiva University (USA).*

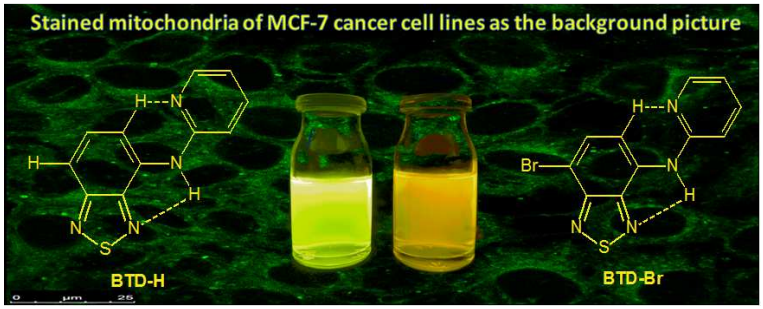

Experimental Section

General. Chemicals and solvents were purchased from commercial sources (Acros or Aldrich) and used without further purification.

X-ray analysis. The molecular structures of **BTD-Br** and **BTD-H** were determined by X-ray diffraction. The X-ray measurements were carried out in a Bruker SMART CCD APEX II area-detector diffractometer with graphite-monochromated Mo $K\alpha$ radiation (λ = 0.71073 Å) at room temperature (T = 293 K).

Mass spectrometry analyses. ESI-MS and ESI-MS/MS measurements were performed in the positive ion mode (*m/z* 50–2000 range) on a Waters Synapt HDMS (high definition mass spectrometer, Manchester, UK) instrument. This instrument has a hybrid quadrupole/ion mobility/orthogonal acceleration time-of-flight (oa-TOF) geometry and was used in the TOF mode, with the mobility cell switched off and working only as an ion guide. All samples were dissolved in acetonitrile or methanol to form 50 μM solutions and were infused directly into the ESI source in a flow rate of 5 μL/min. ESI source conditions were as follows: capillary voltage 3.0 kV, sample cone 30 V, extraction cone 3 V.

NMR analyses. NMR spectra were recorded on a Varian Mercury Plus spectrometer 7.05 T (300 MHz for proton) at room temperature, using a 5-mm internal diameter probe. Deuterated chloroform ($CDCl_3$) and TMS (tetramethylsilane) were used as internal standards.

Infrared analyses. FTIR-ATR spectra were obtained on an Equinox 55 Fourier transform instrument from Bruker. The FTIR-ATR spectra were recorded using a horizontal ATR cell, 7 cm long (10 reflections), from Pike Technologies, covering the 650–4000 cm^{-1} spectral range, using a DTGS detector. Each FTIR-ATR spectrum is the average of 32 scans, using air as reference, at 4 cm^{-1} nominal spectral resolution. All spectra were collected at 21 °C.

Melting point analysis. Melting points were measured on an Electrothermal IA9000 Melting Point apparatus.

Theoretical calculations. All theoretical calculations were carried out using Gaussian 09 suite of programs.[1] Optimizations for ground state (S_0) were performed using the *ab initio* Hartree-Fock (HF) and DFT methods, while the configuration interaction with single excitation (CIS)[2] method was employed to optimize the geometries for first excited state (S_1). According to Brillouin's theorem, CIS method is the HF equivalent for the excited electronic states. The transition states were located using the synchronous transit-guided quasi-Newton QST2 method.[3] Harmonic frequency calculations were performed for every structure to confirm it as a local minimum or transition structures. It is well known that the CIS method could produce reliable geometry but it predicts too high excitation energy.[4] To introduce the dynamic electron correlation, single point energy calculation for the HF and CIS optimized geometries in S_0 e S_1 states has been done at Kohn-Sham DFT[5,6] and its Time-Dependent (TD-DFT)[7] formalism,

respectively, with Beck three-parameters hybrid exchange-correlation functional, known as B3LYP.[8,9] The hybrid method such as DFT//HF or TDDFT//CIS (denoted as single-point calculation//optimization method) has been proved to be an efficient approach in the predicting energy parameters[10,11,12] or optical properties for LED materials.[13,14,15] All calculations were performed using the 6-311+G(2d,p)/LANL2DZ basis set (*i.e.* LANL2DZ pseudo potential for bromine and the 6-311+G(2d,p) split-valence basis set for all other atoms). Absorption spectra in close agreement with experiments have been obtained using the TD-B3LYP/6-311+G(2d,p) level.[16] We calculated partial charges of each atom using CHELPG (Charges from Electrostatic Potentials using a Grid based method).[17]

Cell-imaging experiments. MCF7 cells (breast cancer cells) were plated on 13 mm round glass coverslips on the bottom of 24 wells plate and allowed to adhere for 30 min at 37 ºC in 5% CO_2 atmosphere. Subsequently, non-adherent cells were removed by washing with serum free medium. MCF-7 cells were cultivated in D-MEM medium plus 10% fetal bovine serum at 37ºC in 5% CO_2 atmosphere. After confluence was reached, the culture were washed three times in PBS pH 7.4 and fixed for 15 min in 3.7% formaldehyde solution in PBS at room temperature. The cells were washed three times with PBS and were incubated with markers **BTD-Br** and **BTD-H** diluted 1:1 in DMSO during 30 min at room temperature. As negative control, the cells were incubated at same conditions in PBS. After the incubation time the cells were washed three times with PBS and incubated with TO-PRO-3 (Invitrogen, Oregon/USA) according manufacture recommendations. The coverslips were mounted by using ProLong Gold Antifade (Invitrogen, Oregon/USA) according manufacture recommendations. The samples were analyzed in a Leica Confocal Microscopy TCS SP5. The assays were performed by experimental triplicate in three independents series.

Synthesis of BTD-Br. 4,7-Dibromo-2,1,3-benzothiadiazole[18] (588 mg, 2.0 mmol), $Pd(OAc)_2$ (11. 5 mg, 0.05 mmol), DPEPhos (27 mg, 0.05 mmol), and anhydrous Et_3N (3 mL) were mixed in anhydrous toluene (5 mL) in resealed Schlenk tube. 2-aminopyridine (2.1 mmol) was added to the mixture, and the reaction mixture was stirred at 100 °C for 72 h. The reaction mixture was cooled and filtered through Celite. The Celite was rinsed with ethyl acetate and the mixture solution was concentrated. Purification by column chromatography (EtOAc/hexane mixtures) gave the desired product in 47% yield.

m.p. (°C) = 147-149.

^{1}H-NMR (300 MHz, $CDCl_3$) δ (ppm) = 8.47-8.44 (m, 1H), 8.38-8,36 (m, 1H), 7.84-7.77 (m, 2H), 7.66-7.60 (m, 1H), 6.96-6.88 (m, 2H).

^{13}C-NMR-APT (75 MHz, $CDCl_3$) δ (ppm) = 154.1, 153.0, 148.0, 147.8, 137.7, 134.0, 132.3, 116.5, 111.7, 111.4, 102.5.

IV (KBr, cm^{-1}). 3416, 3018, 2920, 2848, 1592, 1542, 1512, 1481, 1421, 1384, 1151, 1150, 1065, 887, 838, 767.

Synthesis of BTD-H. The dye **BTD-Br** (400 mg, 1.3 mmol) was dissolved in a mixture of 1:9 H_2O:THF. Metallic Mg (13.0 mmol) was added in resealed Schlenk tube and the mixture heated at 100 °C for 24 hours. The reaction mixture was cooled and filtered through Celite. The Celite was rinsed with ethyl acetate and the mixture solution was concentrated. Purification by column chromatography (EtOAc/hexane mixtures) gave the desired product in 23% yield.

m.p. (°C) = 116-118.

^{1}H-NMR (300 MHz, $CDCl_3$) δ (ppm) = 8.41 (d, J = 7.2 Hz, 1H), 8.33 (d, J = 4.8 Hz, 1H), 7.88 (s, 1H), 7.58-7.44 (m, 3H), 6.91 (d, J = 8.1 Hz, 1H), 6.85-6.81 (m, 1H).

^{13}C-NMR-APT (75 MHz, $CDCl_3$) δ (ppm) = 155.0, 154.4, 148.2, 147.8, 137.4, 132.6, 131.5, 116.0, 112.2, 111.4, 110.2.

IV (KBr, cm^{-1}). 3369, 3011, 2922, 2850, 1617, 1588, 1547, 1483, 1362, 1152, 1082, 988, 770, 725.

Table S1. Selected bond lengths (Å) and bond angles (°) for **BTD-Br**.

Br(1)-C(7) 1.889(3)	N(1)-S(2)-N(3) 100.64(1)
S(2)-N(3) 1.616(3)	C(11)-N(16)-C(15) 116.5(3)
S(2)-N(1) 1.617(3)	N(16)-C(11)-N(10) 118.8(3)
N(16)-C(11) 1.323(4)	N(16)-C(11)-C(12) 123.3(3)
N(16)-C(15) 1.344(4)	C(8)-N(1)-S(2) 106.3(2)
N(1)-C(8) 1.346(4)	N(1)-C(8)-C(7) 127.8(3)
N(10)-C(4) 1.382(4)	N(3)-C(9)-C(8) 113.4(3)
N(3)-C(9) 1.344(3)	C(6)-C(7)-Br(1) 122.9(2)
N(10)-C(11) 1.383(4)	C(8)-C(7)-Br(1) 118.9(2)

Table S2. Selected bond lengths (Å) and bond angles (°) for **BTD-H**.

S(2)-N(3) 1.609(4)	N(1)-S(2)-N(3) 100.9(2)
S(2)-N(1) 1.608(4)	C(11)-N(16)-C(15) 116.0(4)
N(16)-C(11) 1.321(6)	N(16)-C(11)-N(10) 118.9(4)
N(1)-C(8) 1.362(6)	N(16)-C(11)-C(12) 123.9(4)
N(10)-C(4) 1.380(5)	C(8)-N(1)-S(2) 106.0(3)
N(3)-C(9) 1.340(5)	N(1)-C(8)-C(7) 126.4(4)
N(16)-C(15) 1.348(6)	N(3)-C(9)-C(8) 113.0(4)
N(10)-C(11) 1.410(6)	C(4)-N(10)-C(11) 128.7(4)
S(2')-N(3') 1.610(4)	C(5)-C(4)-N(10) 128.7(4)
S(2')-N(1') 1.597(4)	N(1')-S(2')-N(3') 101.3(2)
N(16')-C(11') 1.341(6)	C(11')-N(16')-C(15') 115.6(5)
N(1')-C(8') 1.359(6)	N(16')-C(11')-N(10') 118.7(4)
N(10')-C(4') 1.385(6)	N(16')-C(11')-C(12') 124.1(4)
N(3')-C(9') 1.343(6)	C(8')-N(1')-S(2') 106.6(3)
N(16')-C(15') 1.345(6)	N(1')-C(8')-C(7') 127.2(5)
N(10')-C(11') 1.390(6)	N(3')-C(9')-C(8') 113.4(4)
	C(4')-N(10')-C(11') 130.5(4)
	C(5')-C(4')-N(10') 129.0(4)

Table S3. Hydrogen bond distances (Å) and angles (°) in **BTD-Br** and **BTD-H**.

D–H···A	d(D–H)	d(H···A)	d(D···A)	<(DHA)
		BTD-Br		
C(5)–H(5)···N(16)	0.936(1)	2.343(2)	2.971(4)	114.9
N(10)–H(10)···N(3)	0.78(3)	2.39(3)	2.783(4)	113(3)
		BTD-H		
N(10)–H(10)···N(3)	0.95(1)	2.432(2)	2.803(1)	102.9
C(5)–H(5)···N(16)	0.93(0)	2.348(2)	2.933(3)	120.6
N(10')–H(10')···N(3')	0.88(1)	2.383(2)	2.788(2)	108.3
C(5')–H(5')···N(16')	0.93(0)	2.365(1)	2.953(3)	120.9
N(10)–H(10)···N(1')[i]	0.95(4)	2.35(5)	3.283(3)	168(4)

Symmetry operations: [i] x, y, z-1

Table S4. Results of energies (in eV), dipole moment (in D), band gap energy (in eV) and CHELPG partial atomic charges (in *e* units)[a] of the **BTD-Br** and **BTD-H** in both ground and first excited state obtained from B3LYP//HF and TD-B3LYP//CIS, respectively. Values in brackets were obtained by fully optimization at B3LYP/6-311+G(2d,p)/LANL2DZ level of calculation.

Struct.			**Electronic Properties**							
			Energy(eV)	**μ(D)**	**HOMO**	**LUMO**	**ΔE^b**	**$q(N_{10})$**	**q(N3)**	**$q(H_{ESIPT})$**
BTD-Br	**S_0**	**I**	-28678.50595 [28678.68208]	4.2425 [4.4109]	-5.83008 [-5.80342]	-2.50619 [-2.71925]	3.32390 [3.08416]	-0.475 [-0.469]	-0.377 [-0.376]	0.245 [0.246]
		TS	-28676.56215 [-28676.75219]	3.1158 [3.2741]	-5.29238 [-5.27551]	-3.25179 [-3.47710]	2.04060 [1.79841]	-0.848 [-0.819]	-0.162 [-0.180]	0.296 [0.295]
		IV	-28676.76468 [-28676.96699]	4.4309 [4.3414]	-4.99714 [-5.04013]	-3.44390 [-3.61452]	1.55324 [1.42561]	-0.944 [-0.901]	-0.184 [-0.248]	0.341 [0.355]
	S_1	**II**	-28676.13728	4.8899	-5.51307	-2.83300	2.68007	-0.485	-0.399	0.256
		TS*	-28675.25560	3.6991	-5.27442	-3.34431	1.93012	-0.693	-0.222	0.262
		III	-28676.05889	4.9224	-4.84258	-3.70704	1.13554	-0.909	-0.149	0.352
BTD-H	**S_0**	**I**	-28336.76013 [-28336.93321]	2.6252 [2.7768]	-5.77784 [-5.74301]	-2.29421 [-2.50347]	3.48363 [3.23954]	-0.488 [-0.530]	-0.385 [-0.390]	0.244 [0.262]
		TS	-28334.83845 [-28335.02283]	2.4397 [2.4220]	-5.19769 [-5.16884]	-3.03817 [-3.26866]	2.15951 [1.90019]	-0.858 [-0.839]	-0.202 [-0.198]	0.313 [0.302]
		IV	-28335.03538 [-28335.23385]	3.9751 [3.6222]	-4.87822 [-4.91414]	-3.25560 [-3.42321]	1.62263 [1.49092]	-0.943 [-0.923]	-0.242 [-0.268]	0.358 [0.361]
	S_1	**II**	-28334.21122	3.3474	-5.48803	-2.62537	2.86266	-0.510	-0.406	0.252
		TS*	-28333.37650	2.0730	-5.22381	-3.12688	2.09693	-0.742	-0.262	0.288
		III	-28334.25535	4.0655	-4.73455	-3.52717	1.20738	-0.933	-0.314	0.373

[a] *e* = charge of one electron. [b] HOMO-LUMO energies.

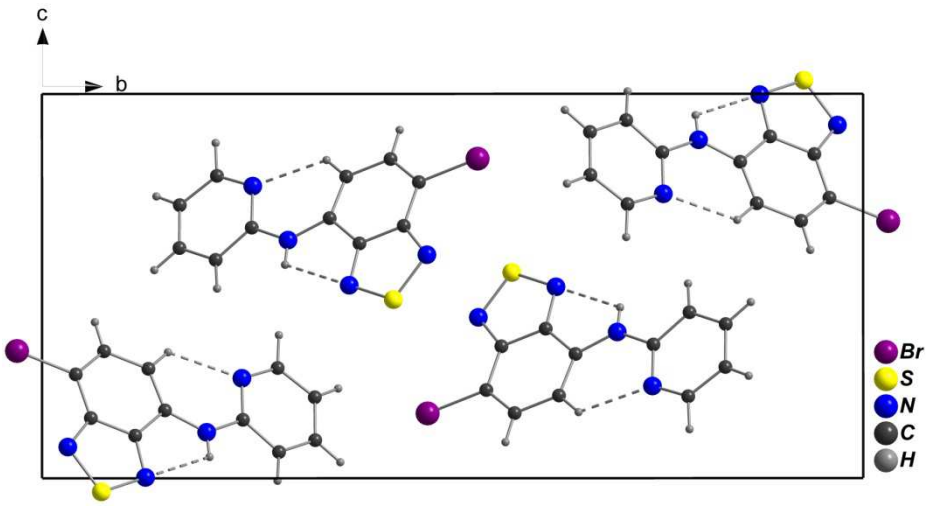

Figure S1. Unit cell of **BTD-Br** showing intramolecular hydrogen bonds, indicated as dashed lines. The packing of molecules in bc plane.

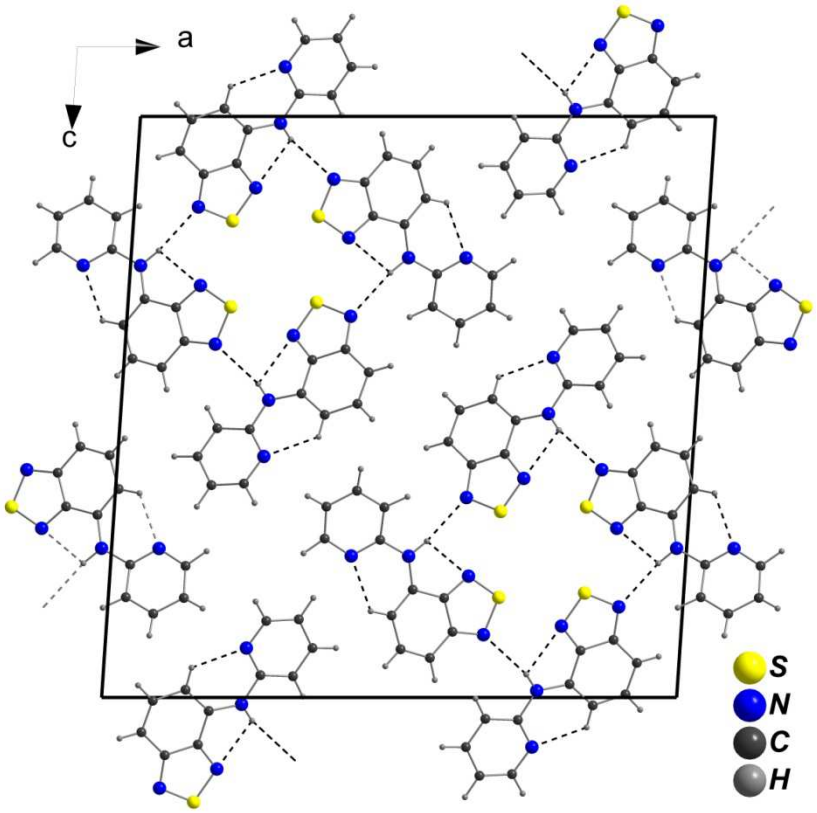

Figure S2. Unit cell of **BTD-H** showing inter and intramolecular hydrogen bonds, indicated as dashed lines. The packing of molecules in ac plane.

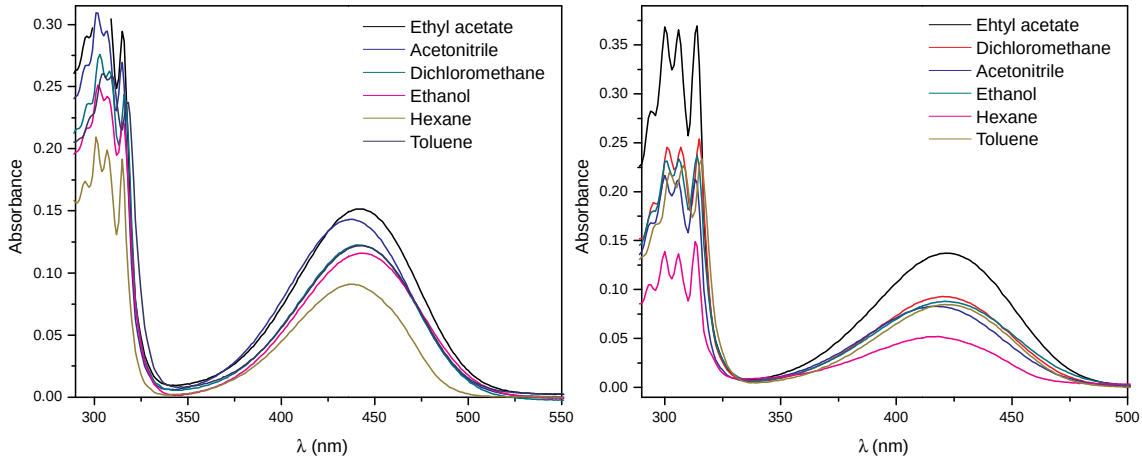

Figure S3. UV-VIS of dyes **BTD-Br** (left) and **BTD-H** (right). Dye concentration of 1.00 x 10^{-5} M in all experiments.

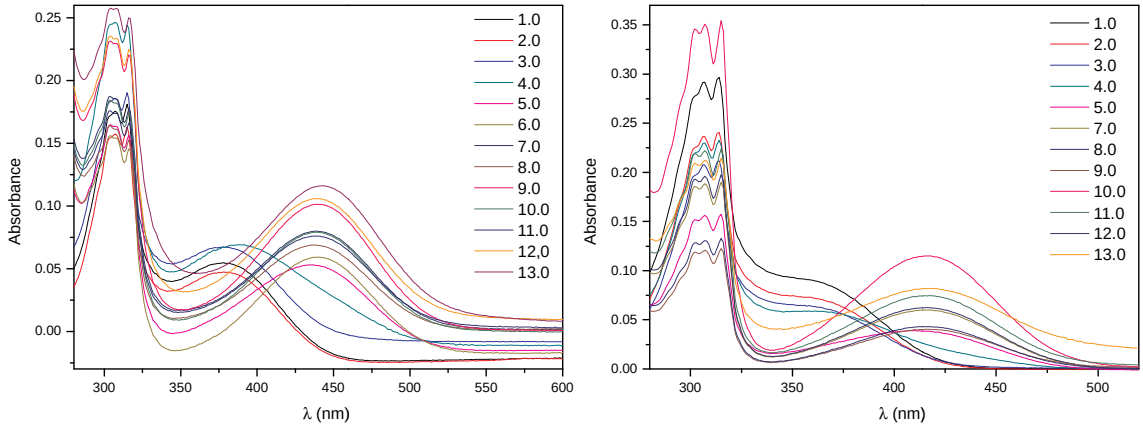

Figure S4. UV-VIS of dyes **BTD-Br** (left) and **BTD-H** (right) at dye concentration of 1.00 x 10^{-5} M at different pH values.

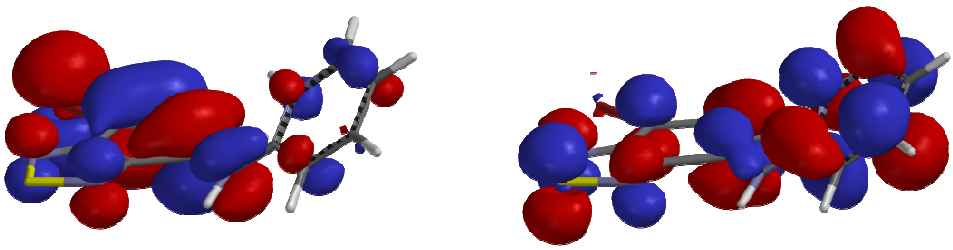

Figure S5. Molecular orbitals as obtained in B3LYP/6-311+G(2d,p)/LANL2DZ level of calculation for **BTD-Br** (cationic). HOMO (left) and LUMO (right).

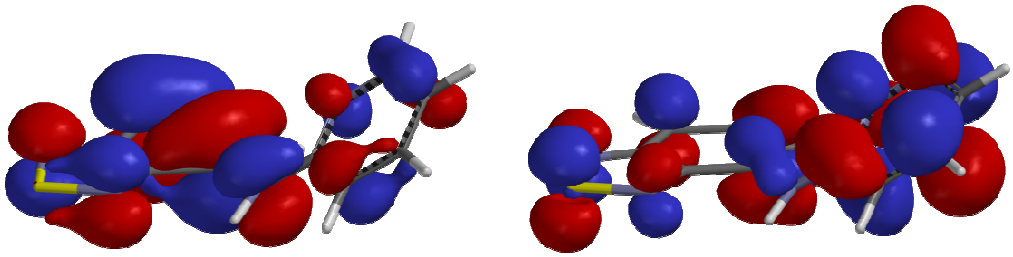

Figure S6. Molecular orbitals as obtained in B3LYP/6-311+G(2d,p)/LANL2DZ level of calculation for **BTD-H** (cationic). HOMO (left) and LUMO (right).

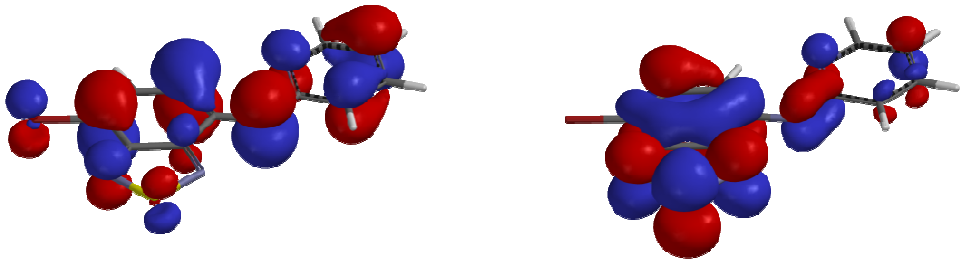

Figure S7. Molecular orbitals as obtained in B3LYP/6-311+G(2d,p)/LANL2DZ level of calculation for **BTD-Br** (anionic). HOMO (left) and LUMO (right).

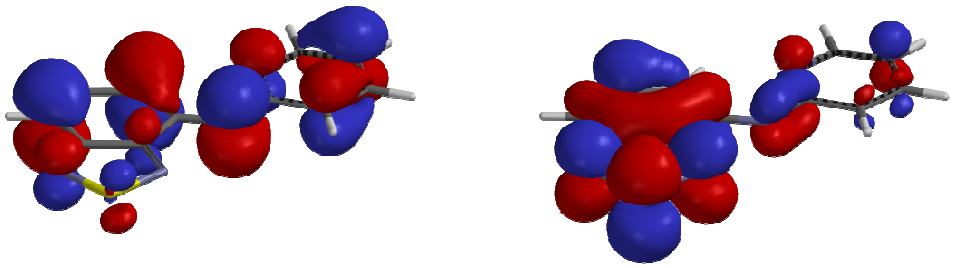

Figure S8. Molecular orbitals as obtained in B3LYP/6-311+G(2d,p)/LANL2DZ level of calculation for **BTD-H** (anionic). HOMO (left) and LUMO (right).

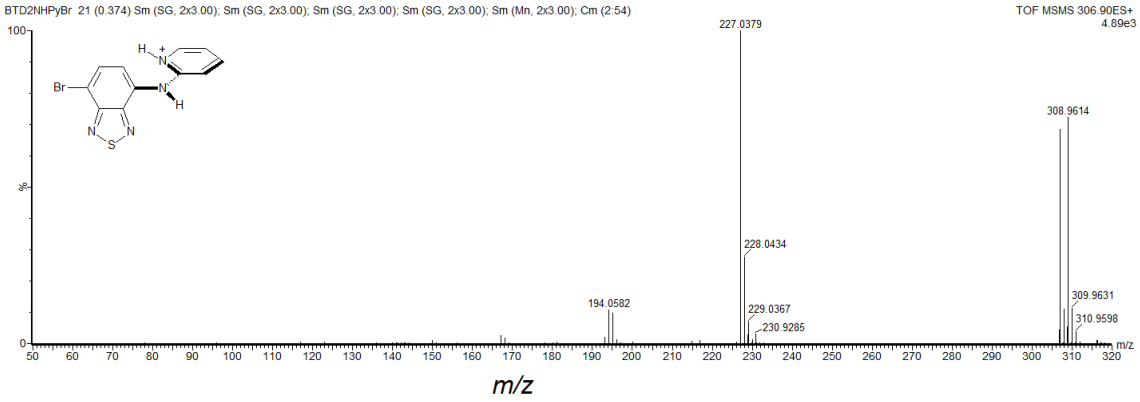

Figure S9. ESI(+)-QTOF product ion spectrum of protonated **BTD-Br**.

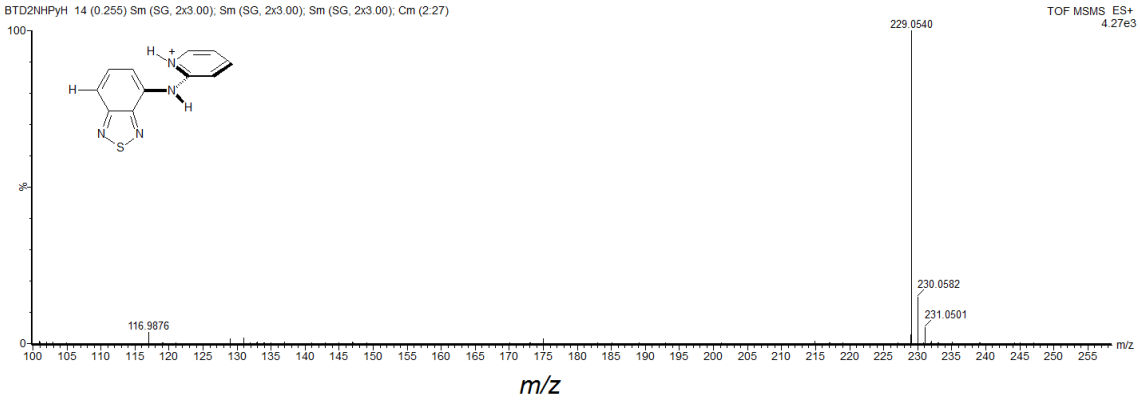

Figure S10. ESI(+)-QTOF product ion spectrum of protonated **BTD-H**.

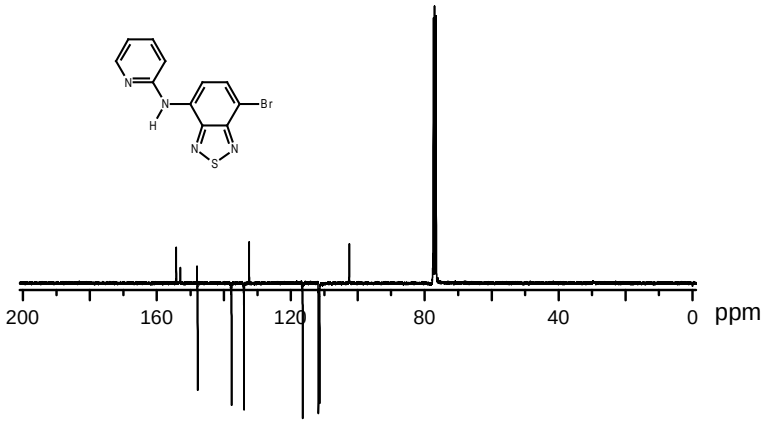

Figure S11. ^{13}C-{^{1}H}-NMR-APT (75 MHz, $CDCl_3$) of **BTD-Br**.

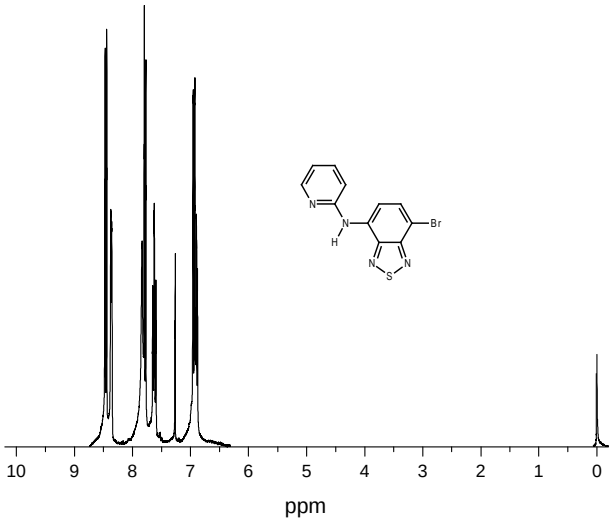

Figure S12. ^{1}H-NMR (300 MHz, $CDCl_3$) of **BTD-Br**.

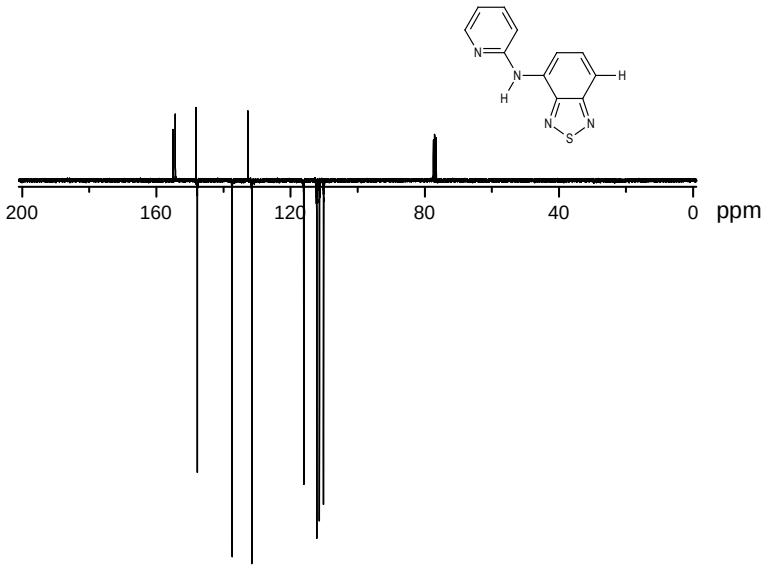

Figure S13. ^{13}C-{^{1}H}-NMR-APT (75 MHz, $CDCl_3$) of **BTD-H**.

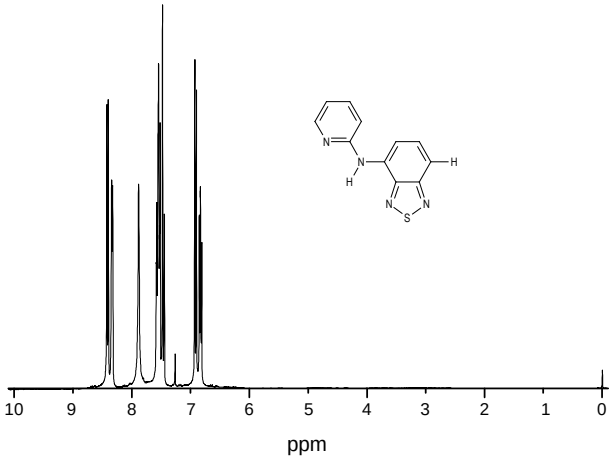

Figure S14. ^{1}H-NMR (300 MHz, $CDCl_3$) of **BTD-H**.

References

[1] M. J. Frisch, G. W. Trucks, H. B. Schlegel et al., GAUSSIAN 09, Revision A.02, Gaussian, Inc., Wallingford CT, 2009.

[2] J.B. Foresman, M. Head-Gordon, J.A. Pople, M.J. Frisch, *J. Phys. Chem.*, 1992, **96**, 135-149.

[3] C. Peng, H. B. Schlegel, *Israel J. of Chem.*, 1993, **33**, 449-454.

[4] Z. Yang, S. Yang, J. Zhang, *J. Phys. Chem. A*, 2007, **111**, 6354-6360.

[5] P. Hohenberg, W. Kohn, *Phys. Rev.*, 1964, **136**, B864-B871.

[6] W. Kohn, L. Sham, *J. Phys. Rev.*, 1965, **140**, A1133-A1138.

[7] E. Runge, E. K. U. Gross, *Phys. Rev. Lett., 1984,* **52**, 997-1000.

[8] A.D. Becke, *J. Chem. Phys.*, 1993, **98**, 5648-5652.

[9] C. Lee, W. Yang, R.G. Parr, *Phys. Rev. B*, 1998, **37**, 785-789.

[10] L. R. Domingo, M. T. Picher, R.J. Zaragozá, *J. Org. Chem.*, 1998, **63**, 9183-9189.

[11] M. K. Shukla, J. Leszczynski, *Int. J. Quantum Chem.*, 2005, **105**, 387-395.

[12] R. Jin, J. Zhang, *Theor. Chem. Acc.*, 2009, **124**, 339-344.

[13] M. Sun, B. Niu, J. Zhang, *J. Mol. Struct: Theochem*, 2008, **862**, 85-91.

[14] M. D. Halls, H. B. Schlegel, *Chem. Mater*., 2001, **13,** 2632-2640.

[15] B. Hu, G. Gahungu, J. Zhang, *J. Phys. Chem*. A, 2007, **111**,4965-4973.

[16] T. L. Fonseca, H. C. B. de Oliveira, M. A. Castro, *Chem. Phys. Lett.*, 2008, **457**, 119-123.

[17] C. M. Breneman, K. B. Wiberg, *J. Comput. Chem.*, 1990, **11**, 361-373.

[18] F. S. Mancilha, B. A. D. Neto, A. S. Lopes, P. F. Moreira, F. H. Quina, R. S. Goncalves, J. Dupont, *Eur. J. Org. Chem.*, 2006, 4924-4933.